

**CORRELATIONS FOR HEAT GENERATION AND OUTER RING TEMPERATURE
OF HIGH SPEED AND HIGHLY LOADED BALL BEARINGS IN AN AERO ENGINE**

**KORRELATIONEN FÜR DIE WÄRMEENTWICKLUNG UND DIE AUSSENRING-
TEMPERATUR IN SCHNELLDREHENDEN UND HOCHBELASTETEN KUGEL-
LAGERN EINES FLUGTRIEBWERKS**

DR. MICHAEL FLOUROS

MTU AERO ENGINES, AIR AND OIL SYSTEMS GROUP, DACHAUER STR. 665,
80995 MUNICH, GERMANY

Email address: Michael.flouros@muc.mtu.de

Tel: +49-89-14899192, Fax: +49-89-148995341

ABSTRACT

Advanced aircraft engine development in recent years has dictated increased rotational speeds with the consequence of increased mechanical stress requirements for rolling element bearings. A vast amount of heat is rejected which results in high oil scavenge and bearing metal temperatures. A ball bearing and its associated chamber from an RB199 turbofan Engine were used in an experimental investigation to determine the impact of several operating parameters on the scavenge and bearing race temperatures. The test bearing was a 124mm PCD ball bearing with a split inner-ring employing under-race lubrication by two individual jets providing oil through each half of the inner-ring. The bearing run over a wide range of D times N (DN) values ranging from 0.3×10^5 to 2.1×10^6 rpm x mm with D the bore diameter of the bearing. The direction of the oil ingestion in the bearing (for or against the direction of the axial load) was found to have a considerable effect to the oil distribution

and consequently to the heat generation in it. A significant reduction in the heat to oil was achieved when the oil was fed at certain proportions (ratio) by the two nozzles.

Heat to Oil and Outer ring metal temperature correlations which consider the influence of the direction of oil ingestion relative to the direction of the axial load have been developed and compared to test results.

This work is part of the European Research programme Brite Euram ATOS (Advanced Transmission and Oil Systems).

ZUSAMMENFASSUNG

Die Forderung nach besser werdendem Kreisprozesswirkungsgrad hat in den letzten Jahren bei Flugtriebwerken dazu geführt, dass die Drehzahlen der Rotoren ständig ansteigen mit der Folge, dass auch die Lebensdauieranforderungen für die Triebwerkswälzlager ansteigen. Bedingt durch die höhere Beanspruchung der Wälzlager erreicht das für die Lagerschmierung verwendete Öl sehr hohe Austrittstemperaturen. Zudem führt die höhere Beanspruchung zu höheren Materialtemperaturen im Lager. Im Rahmen der nachfolgenden experimentellen Untersuchung wurden ein Originalkugellager und eine Originallagerkammer aus dem RB199 Triebwerksprogramm herangezogen. Das Testkugellager hat einen Teilkreisdurchmesser von 124mm und besitzt einen geteilten Innenring. Für die Schmierung wurden zwei Düsen eingesetzt, die das Öl jeweils durch die zwei Hälften des Innenrings in das Lager leiteten. Das Kugellager wurde im $D \times N$ -Bereich zwischen 0.3×10^5 bis 2.1×10^6 rpm \times mm betrieben. D ist hier der Innenringdurchmesser (Wellendurchmesser) von 102.5mm des Lagers und N ist die Drehzahl. Abhängig davon, wie das Öl in das Lager eingespritzt wurde (in Richtung bzw. in Entgegengesetzter Richtung zur wirkenden Lageraxiallast) und zu welchen

Proportionen dies geschah, gab es einen signifikanten Einfluss auf die Wärmebelastung des Öls.

Diese Arbeit wurde im Rahmen des Europäischen Forschungsprogramms Brite Euram ATOS (Advanced Transmission and Oil Systems) durchgeführt.

Keywords: Ball Bearing, Heat to Oil, Metal Temperature, Correlations, Design Guidelines

Schlüsselwörter: Kugellager, Wärmeproduktion, Metalltemperatur, Korrelationen, Auslegungsrichtlinien

NOMENCLATURE

c_{pFS} = Mean specific heat Capacity [KJ/Kg K]

Front Scavenge

c_{pRS} = Mean specific heat Capacity [KJ/Kg K]

Rear Scavenge

D = Bore diameter= 102.5 [mm]

F_{ax} = Axial Load [KN]

HTO = Heat To Oil [W]

m = Total mass flow = $m_{FS} + m_{RS}$ [Kg/s]

m_{FS} = Front Scavenge mass flow [Kg/s]

m_{RS} = Rear Scavenge mass flow [Kg/s]

N = Rotational Speed [rpm]

p = Pressure [bar]

PCD = Pitch Circle Diameter	[mm]
Q = Heat to Oil (HTO)	[KW]
T = Temperature	[°C]
T _A = Front Scavenge Temperature	[°C]
T _B = Rear Scavenge Temperature	[°C]
TOI = Oil Inlet Temperature	[°C]
TOR = Outer Ring Temperature	[°C]
V = Total Oil Flow = V _{Front} + V _{Rear}	[L/H]
V _{Front} = Oil Flow through Front jet	[L/H]
V _{Rear} = Oil Flow through Rear jet	[L/H]
X = Oil flow Ratio = Ratio of oil through front Jet to the total oil flow in the bearing	
v = kinematic viscosity of the oil at inlet temperature (TOI)	

INTRODUCTION

Highly loaded bearings generate heat in the contact areas between the rolling elements and the race, the rolling elements and the cage and in the annular gaps between the cage and the races. The generated heat is caused by friction in the contact areas and by churning/windage as a result of dissipation of Euler work (acceleration to circumferential speed). Oil is usually supplied to rolling elements via the under-race lubrication method. Whereas only a very small amount of oil is used for lubrication most of it is used to remove the heat from the bearing. The main objective in the ATOS programme was to reduce power losses by using screens around a ball bearing in a vented chamber [4]. Within the scope of this research the impact of the operating parameters affecting the power losses in the bearing

chamber were investigated [2]. These were the oil and sealing air flow, the temperature, the axial load, the rotor speed, the bearing chamber pressure and the split of the oil flow at any ratio through the inner ring. The wealth of information about power losses in bearings is specifically reflected in [1], [5], [6], [7], [8], [9], [10], [11], and [12]. During testing a considerable temperature difference of the oil leaving the bearing from both sides was detected. This implied the presence of a non uniform distribution of the oil in the bearing [3]. Results showed minimum heat generation in the bearing when about 25% of the oil was supplied through the unloaded side of the inner-ring. The correlations presented herein are the first of this kind which take into account the direction of the oil ingestion relative to the direction of the axial load. They have demonstrated very good agreement with results from bearings with bore diameters ranging from 40mm to 120mm, a rotor speed range between 6000rpm and 24000rpm and up to 25KN of axial load.

RIG DESCRIPTION / INSTRUMENTATION

Schematics of the test facility and the bearing chamber are shown in Figures 1 and 2. The ball bearing (Figure 2) has an inner land riding cage with a split inner ring and under-race lubrication was applied. Each half of the inner ring has eighteen 1mm holes which centrifugally direct the oil to the cage scoop and from there to the rolling elements. Two additional 1mm holes on each half of the inner-ring are used for guiding the cage. The cage guiding holes are at a circumferential distance of 180° to each other and are placed towards the edge of the inner ring so that they face the cage land. The bearing has 22 rolling elements with a diameter of 14mm. The material of the bearing inner and outer race is M50 steel. The supplier of the bearing is FAG Kugelfischer.

The oil is delivered by two individual nozzles (Figure 1, Figure 2) and the flow through each of them is adjustable so that the bearing can be lubricated at any flow ratio X . This is defined as the ratio of the oil flow from the nozzle which supplies the unloaded half of the inner ring (V_{Front}) to the total oil flow (V):

$$X = V_{Front} / V \quad \text{with } V = V_{Front} + V_{Rear}$$

The bearing chamber is sealed by air as this is shown in Figure 2. Since the impact of the sealing air on the parasitic losses in a bearing chamber is known [2], in order not to affect the quality of the results, a very small quantity of air at oil inlet temperature was introduced into the chamber just in order to avoid oil migration through the seal (gap ring). The pressure in the chamber was maintained 2-4KPa above the ambient pressure.

Thermocouples were used to monitor the heat rejection from the bearing (Figure 2). Two rows of three circumferential thermocouples T_A and T_B were placed adjacent to the bearing in the gap between the outer ring and the rotating cage on each side. Their circumferential distance was 120° on each side. T_A and T_B recorded the temperatures of the hot scavenge oil leaving the bearing through the gap between the outer ring and the cage as this was recorded during bearing operation at several operating conditions using an Endoscope (Figure 2) and a High Speed camera [4]. Two additional rows of thermocouples, which are not shown in Figure 2, were placed at a distance of 1cm from each side of the bearing for additional monitoring. Three circumferential thermocouples (TOR) were also placed at a distance of 120° in the outer ring material adjacent to the loaded side. TOR thermocouples recorded the material temperature of the outer ring. The scatter of the flow measurements was $\pm 1.5\%$ of the average flow and less than $\pm 1\%$ for the temperature.

The oil flow was varied between 15L/H and 450L/H, the temperatures for air and oil were varied up to 130°C , the rotational speed was between 6000rpm and 19000rpm

and the axial load was between 4KN and 22KN. A lubricant meeting the MIL-PRF-23699 standard was used (Mobil Jet II).

CORRELATIONS AND RESULTS

The oil flow distribution in the bearing was found to depend on the oil flow ratio X (Figure 3, [3]). At $X=0$ (only the rear nozzle is active) the rear scavenge flow is the highest (about 80% of the total flow) but still an amount of 20% is transmitted through the bearing. On the contrary at $X=1$ (only the front nozzle is active) the front scavenge flow is about 55% of the total flow whereas about 45% are transmitted through the bearing. As already mentioned the measurement of each of the temperatures T_{OR} , T_A and T_B was performed with three circumferential thermocouples. For the calculation of the heat rejection into the oil, the average values for T_A and T_B were used. The scatter of T_A and T_B around the average value was less than $\pm 2^\circ\text{C}$. The same is also valid for T_{OR} .

Figure 4 depicts for a certain operating condition T_{OR} , T_A and T_B as a function of the oil flow ratio X . T_{OR} and the front scavenge temperature T_A are decreasing with X whereas the rear scavenge temperature T_B rises. This behaviour was observed throughout the testing. A maximum temperature difference of about 76°C between T_A and T_B was recorded when the bearing was lubricated by only the front nozzle ($X=1$) at the displayed conditions. Using the measured scavenge temperatures and the scavenge flows the heat which is transferred from the bearing to the oil (Heat to Oil) can be calculated.

This is defined as:

$$\text{HTO} = Q = m_{FS} \cdot c_{pFS} \cdot (T_A - \text{TOI}) + m_{RS} \cdot c_{pRS} \cdot (T_B - \text{TOI})$$

c_{pFS} and c_{pRS} are the mean specific heat capacities. They are average values between the specific heat capacities at the front and the rear and at oil inlet

respectively. m_{FS} and m_{RS} are the front and rear scavenge mass flows (i.e. the oil that leaves the bearing from each side) and T_A , T_B are the corresponding scavenge temperatures (Figure 2). Figure 5 shows for three rotational speeds the Heat to Oil (Q) as a function of X. At $X \sim 0.25$ a minimum value is reached. In the case of 19000rpm the difference in HTO between the minimum point ($X \sim 0.25$) and the peak value ($X=1$) is about 15% of the maximum value [3]. Figure 6 shows for the same conditions the outer ring temperatures TOR as a function of X.

In order to create the correlations more than 1000 test results were processed. These correlations consider the parameters which affect the heat generation and consequently the outer ring temperature of the bearing:

$$(1) \quad Q = E D^\alpha N^\beta v^\gamma F_{ax}^\delta V_{oil}^\epsilon (A X^2 + B X + C)^\zeta \text{ for the Heat to Oil with Q in KW and}$$

$$(2) \quad TOR = G D^\eta N^\theta v^\kappa F_{ax}^\lambda V_{oil}^\mu (1+X)^\xi + TOI \text{ for the outer ring temperature in}$$

Celsius. The coefficients A, B, C, E, G and the exponents α , β , γ , δ , ϵ , ζ , η , θ , κ , λ , μ , ξ can be estimated iteratively when (1) and (2) are brought into a linear form. This can be achieved by using logarithmic functions:

$$\begin{aligned} \text{Log}_{10} (Q) &= \text{Log}_{10} [D^\alpha N^\beta v^\gamma F_{ax}^\delta V_{oil}^\epsilon (A X^2 + B X + C)^\zeta] + \text{Log}_{10} (E) \\ &= \text{Log}_{10} (GL1) + \text{Log}_{10} (E) \end{aligned} \quad (3)$$

with $GL1 = D^\alpha N^\beta v^\gamma F_{ax}^\delta V_{oil}^\epsilon (A X^2 + B X + C)^\zeta$ and

$$\text{Log}_{10} (TOR - TOI) = \text{Log}_{10} [D^\eta N^\theta v^\kappa F_{ax}^\lambda V_{oil}^\mu (1+X)^\xi] + \text{Log}_{10} (G) \quad \text{or}$$

$$\text{Log}_{10} (TOR - TOI) = \text{Log}_{10} (GL2) + \text{Log}_{10} (G) \quad (4)$$

with $GL2 = D^\eta N^\theta v^\kappa F_{ax}^\lambda V_{oil}^\mu (1+X)^\xi$

All constants and the exponents were determined iteratively by using a best fit algorithm. Table 5 summarizes the derived coefficients and exponents. The final forms of the equations are:

$$Q = 1.50674 \times 10^{-9} D^{1.11} N^{1.3855} v^{0.0525} F_{ax}^{0.2152} V_{oil}^{0.3831} (2,25X^2 - 1,5068X + 7,0221)^{0.761}$$

(5) and

$$TOR = 1.1506 \times 10^{-3} D^{0.8729} N^{0.9876} V_{oil}^{-0.3174} v^{0.1234} F_{ax}^{0.2469} (1+X)^{-0.3174} + TOI \quad (6)$$

Ninety two percent of the measured values for the outer ring temperature (Figure 7) are in a range of $\pm 10^\circ\text{C}$ from the values predicted by Equation 6 whereas 90% of the heat to oil values is within the $\pm 15\%$ range. A comparison of test and derived results from Equations 5 and 6 is shown in Tables 1-4.

As can be seen from these Tables the correlations yield results which are in a very good agreement with the experimental results. The very good accuracy of the correlations was proven when these were applied on bearings with bore diameters of 40mm and 120mm which were from different programmes and were running at speeds up to 24000rpm and axial loads up to 25KN.

In order to check whether the exponents in the correlations are physically reflecting the impact of the operating parameters a survey was initiated on the basis of Equation 5 and the results were compared and discussed with results derived by the bearing manufacturer FAG Kugelfischer in Germany. Using Equation 5 the heat generation was calculated for the test bearing (102.5mm bore diameter bearing) as a function of the rotational speed. Then for a rotational speed of 19000rpm the bearing bore diameter was varied from 102.5mm down to 42.5mm. Based on the FAG experience the heat generation increases with the rotational speed at a rate of change of approximately the ratio of the higher to the lower speed to the exponent of 1.50. There, the heat generation is dictated by the rolling and the slip friction in the contact areas and of course by the centrifugal force which increases with the square rotational speed. On the contrary the increase of the bore diameter of the bearing leads to an approximately linear but steeper increase of the heat generation

compared to the case before. This is because the number and the size of the rolling elements increase hence contributing to higher centrifugal forces, friction and churning. In reality the mechanism of heat generation in bearings is very complex.

Figure 8 depicts results derived by FAG and also with Equation 5 on the basis of the test bearing (Figure 2). The reference value is the peak value by Equation 5 at 19000rpm. The trends shown on the corresponding curves in Figure 8 are very similar. This is a good indication that the exponents in Equation 5 adequately reflect the physics of heat generation in the ball bearing. The upper curves in Figure 8 depict the bore diameter variation at a constant speed of 19000rpm whereas the lower curves are at a constant bore diameter of 102.5mm (test bearing) with the speed varying from 7000rpm to 19000rpm. The scatter in the absolute values between FAG and Equation 5 is something that was expected since the measuring methods differ from each other. MTU has measured the oil scavenge temperatures adjacent to the bearing from both sides whereas FAG has recorded the common scavenge temperature downstream of the sump of the bearing chamber in the scavenge line. In this case other thermal impacts from the environment like for example the chamber walls or the sealing air, are possible and always can have an impact on the final result. Additionally only the MTU correlation can take into account the direction of ingestion of the oil (oil flow ratio X) which affects the flow distribution in the bearing.

There are few additional observations that can be of value: With increasing oil viscosity which can result by the use of oil brands with a higher viscosity, the bearing operating temperature TOR and the heat Q which is rejected into the oil both increase. This is because of two basic reasons: a decrease in the film heat transfer coefficient which reduces the heat transfer from the bearing surfaces hence leading to the higher TOR and an increase in the heat developed by the shearing of oil with a

higher viscosity hence resulting to higher churning losses and heat rejection into the oil.

PROPOSED LIMITATIONS AND DESIGN GUIDELINES

The following limitations and design guidelines should be considered when the correlations are applied in order to achieve the best end result:

Limitations:

Rotational Speed: $6000\text{rpm} \leq N \leq 24000 \text{ rpm}$

Bore Diameter: $40\text{mm} \leq D \leq 120 \text{ mm}$

D x N: $0.24 \times 10^6 - 2.9 \times 10^6 \text{ rpm x mm}$

Axial Load: $F_{ax} \leq 25 \text{ KN}$

Oil Flow: $50\text{L/H} \leq V_{oil} \leq 450 \text{ L/H}$

Oil Inlet Temperature: $30^\circ\text{C} \leq \text{TOI} \leq 130^\circ\text{C}$

Guidelines:

- When about 25% of the oil is supplied to the bearing through the unloaded side of the inner-ring then the heat generation reduction can be about 15%.
- At the lubrication system design phases an assessment of the oil flow and the heat generation into the bearing is required. This can be accomplished by defining the operating conditions of the bearing like maximum rotational speed, axial load and possible oil inlet temperature. Then using Equation 5 a diagram of the generated heat Q against the oil flow should be created (Figure 9). From Q the mean oil temperature from the bearing can be calculated (Figure 10). The design point for the bearing lubrication is there where the rate of change of the oil temperature from the bearing gets small. Figure 10 depicts the oil temperature from the bearing as a function of the oil flow. In this case the design

point would be at 250L/H which yields a mean oil temperature from the bearing of 143°C with the neighbouring points only deviating by 2-3°C.

- The bearing outer race temperature can then be calculated with Equation 6. For the referenced design point the outer race temperature is about 163°C.
- When an oil flow rate of more than 250L/H is selected this would considerably increase the secondary power losses in the bearing chamber by adding churning and Windage; therefore this should be avoided [2].
- At 250L/H the bearing is lubricated satisfactory and neither the mean oil temperature from the bearing nor the bearing outer race temperatures are excessive. Oil temperatures above 200°C should be avoided since the oil coking temperature of 230°C can easily be reached after engine shut off particularly in the hot sections of the engine as a result of thermal radiation (soak back). Bearing outer race temperatures should follow the rule for the same reason but additionally moderate bearing race temperatures extend bearing life.

CONCLUSIONS

Based on a vast amount of experimental results, correlations for predicting the heat to oil and the outer ring temperature at the loaded side of the outer ring of the bearing have been developed. These demonstrated very good accuracy to the test results.

These correlations are the first of this kind which take into account the direction of oil ingestion relatively to the direction of the axial load. They have also been proven when extended for bearings with bore diameters ranging between 40mm and 120mm.

Minimum heat generation is achieved when about 25% of the lubricant is supplied to the bearing through the unloaded side of the inner-ring.

A comparison of the heat generation results from Equation 5, with the results derived by the bearing manufacturer FAG Kugelfischer, assuming the same operating conditions, have shown similar behaviour. This was a good indication that the coefficients and exponents used in the correlations reflect the physical heat generation characteristics.

The FAG results are very satisfactory for the designer however the FAG correlation is not in the public literature. The MTU proposed correlations are a step further since they take into account the direction of the oil ingestion which affect the flow management in the bearing. The measurement of the oil temperatures adjacent to the bearing from both sides has lead to a higher accuracy.

ACKNOWLEDGEMENT

The author would like to express his acknowledgement to the European Commission for the financial support within the GROWTH Programme, Research Project 'Advanced Transmission and Oil System Concepts (ATOS)', contract G4RD-CT-2000-00391. Also the author wishes to acknowledge the expert support and advice from FAG Kugelfischer.

REFERENCES

- [1] G. E. Clarke, H. H. Mabie, Prediction of the Running Torque of Instrument Ball Bearings at High Speed Under Combined Radial and Axial Loads, Lubrication Engineering, July 1970, pp. 236-242
- [2] M. Flouros, The Impact of Oil and Sealing Air Flow, Chamber Pressure, Rotor Speed and Axial Load on the Power Consumption in an Aeroengine Bearing Chamber, Journal of Engineering for Gas Turbines and Power, Vol. 127, January 2005, pp.182-186.

- [3] M. Flouros, Oil Pumping Action in High Speed and High Loaded Ball Bearings, GT2004-53406, ASME Turbo Expo, Vienna, Austria, 2004
- [4] M. Flouros, Reduction of Power Losses in Bearing Chambers using Porous Screens Surrounding a Ball Bearing, Journal of Engineering for Gas Turbines and Power, Vol. 128, January 2006, pp. 178-182
- [5] T. A. Harris, Rolling Bearing Analysis, Fourth Edition, John Wiley & Sons, Wiley-Interscience, 2001
- [6] Z.N. Nemeth, E.F Macks, W. J. Anderson, Investigation of 75-Millimeter-Bore Deep-Groove Ball Bearings under Radial Load at High Speeds, Oil-Flow-Studies, NACA Technical Note 2841, December 1952
- [7] Z.N. Nemeth, E.F Macks, W. J. Anderson, Influence of Lubricant Viscosity on Operating Temperatures of 75-Millimeter-Bore Cylindrical Roller Bearings at high speeds, NACA Technical Note 2636, 1952
- [8] H. W. Scibbe, H. E. Munson, Experimental Evaluation of 150-Millimeter Bore Ball Bearings to 3-Million DN using either Solid or Drilled Balls, Transactions of the ASME, Journal of Lubrication Technology, Paper No. 73-Lub-19, 1973.
- [9] H. Signer, E. N. Bamberger, E. V. Zaretsky, Parametric Study of the Lubrication of Thrust Loaded 120-MM Bore Ball Bearings to 3 Million DN, Transactions of the ASME, Journal of Lubrication Technology, Paper No. 73-Lub-24, 1973.
- [10] H. Styri, Friction Torque in Ball and Roller Bearings, Mechanical Engineering, Vol. 62, 1940, pp. 886-890
- [11] D.P. Townsend, C. W. Allen, E.V. Zaretsky, Study of Ball Bearing Torque Under Elastohydrodynamic Lubrication, Journal of Lubrication Technology, Transactions of the ASME, Series F, Vol. 96, October 1974, pp. 561-571

- [12] R. J. Trippet, A High-Speed Rolling Element Bearing Loss Investigation, Transactions of the ASME, Journal of Engineering and Power, Vol. 100, January 1978.

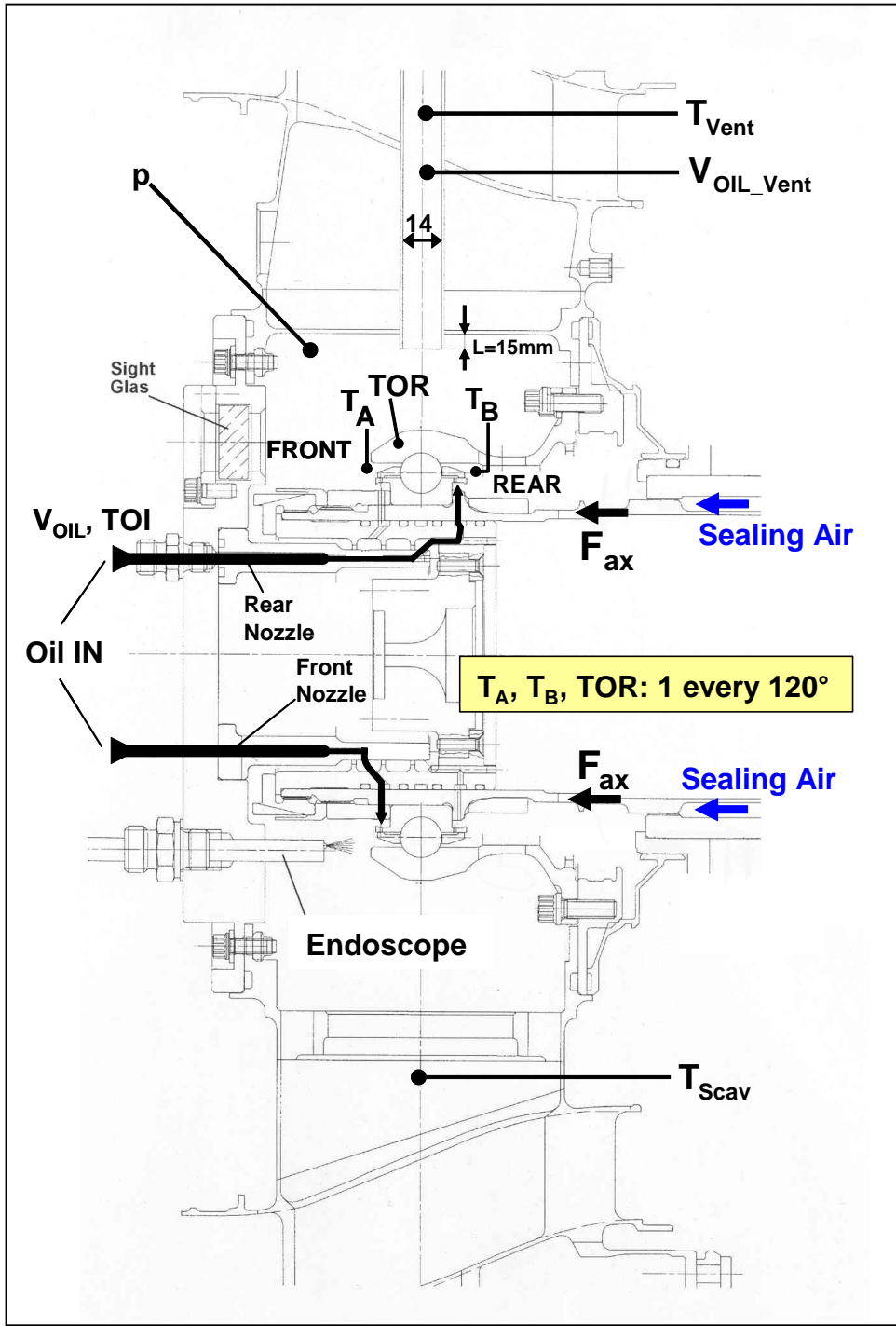


Figure 2. Schematic of the Bearing Chamber and the Ball Bearing

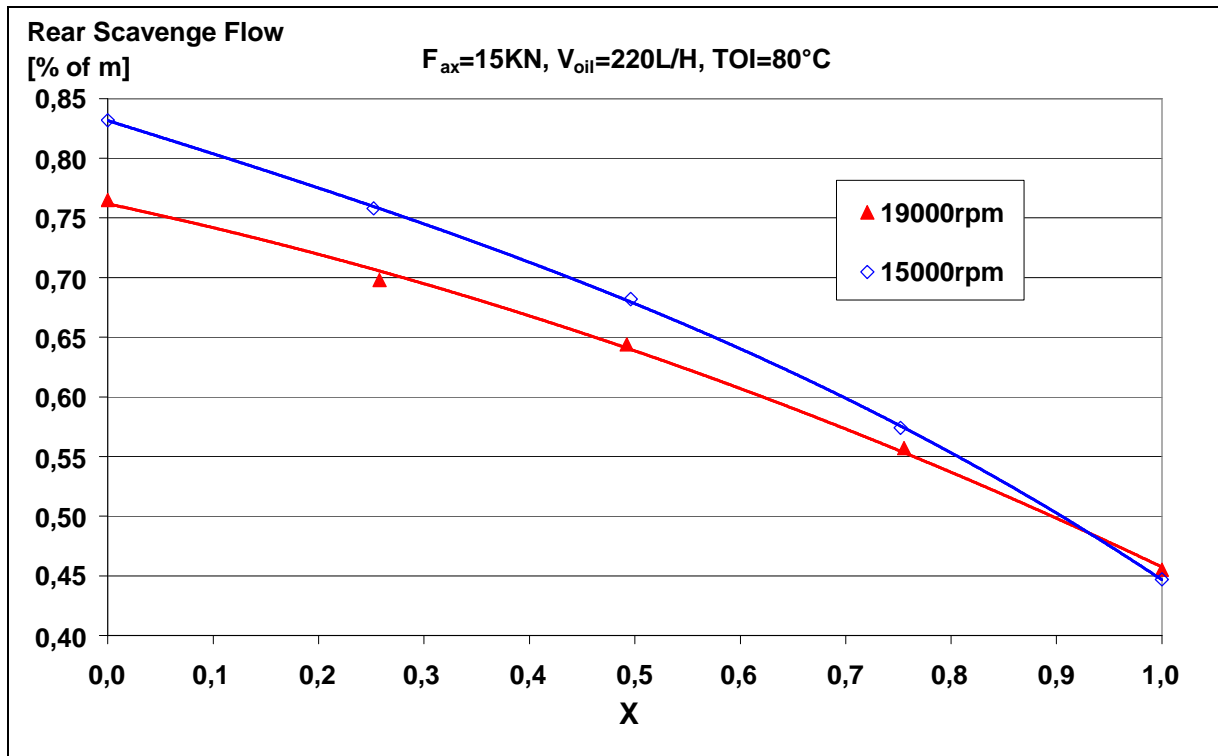


Figure 3. Rear Scavenge oil flows as a function of the oil flow ratio X and different rotational speeds

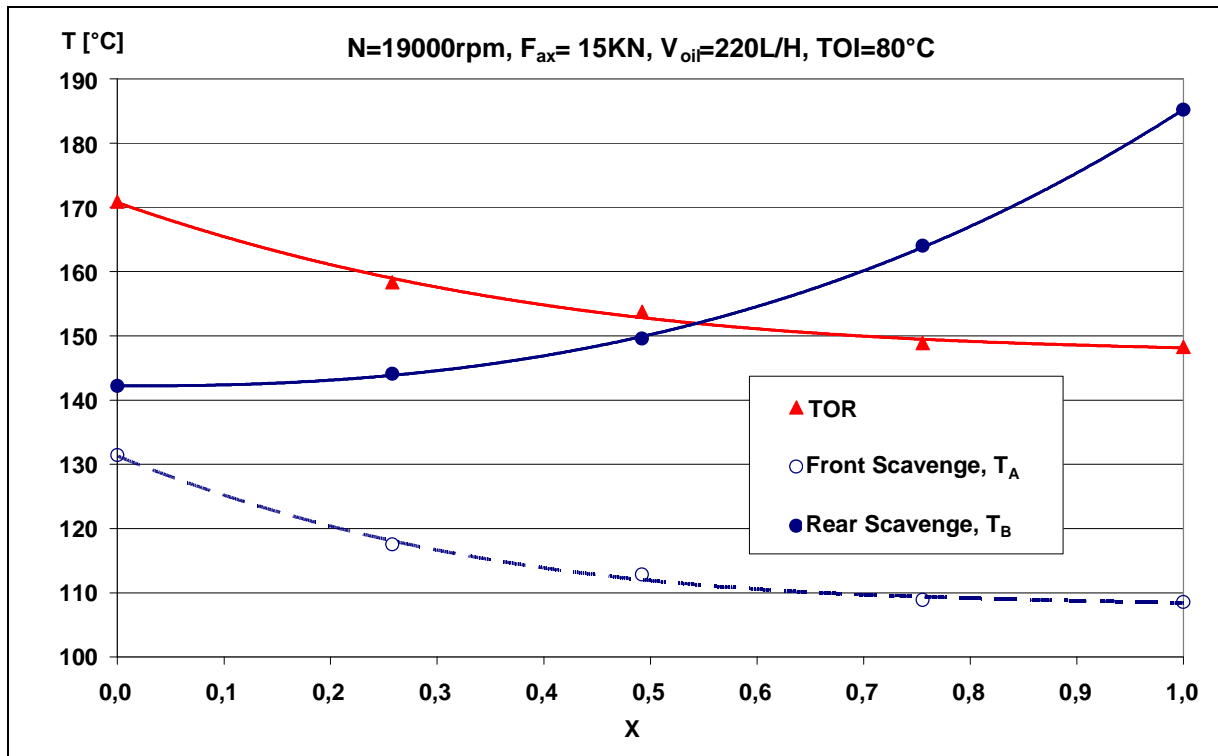


Figure 4. Rear, Front Scavenge and Outer Ring temperatures as a function of the oil flow ratio X at 19000rpm

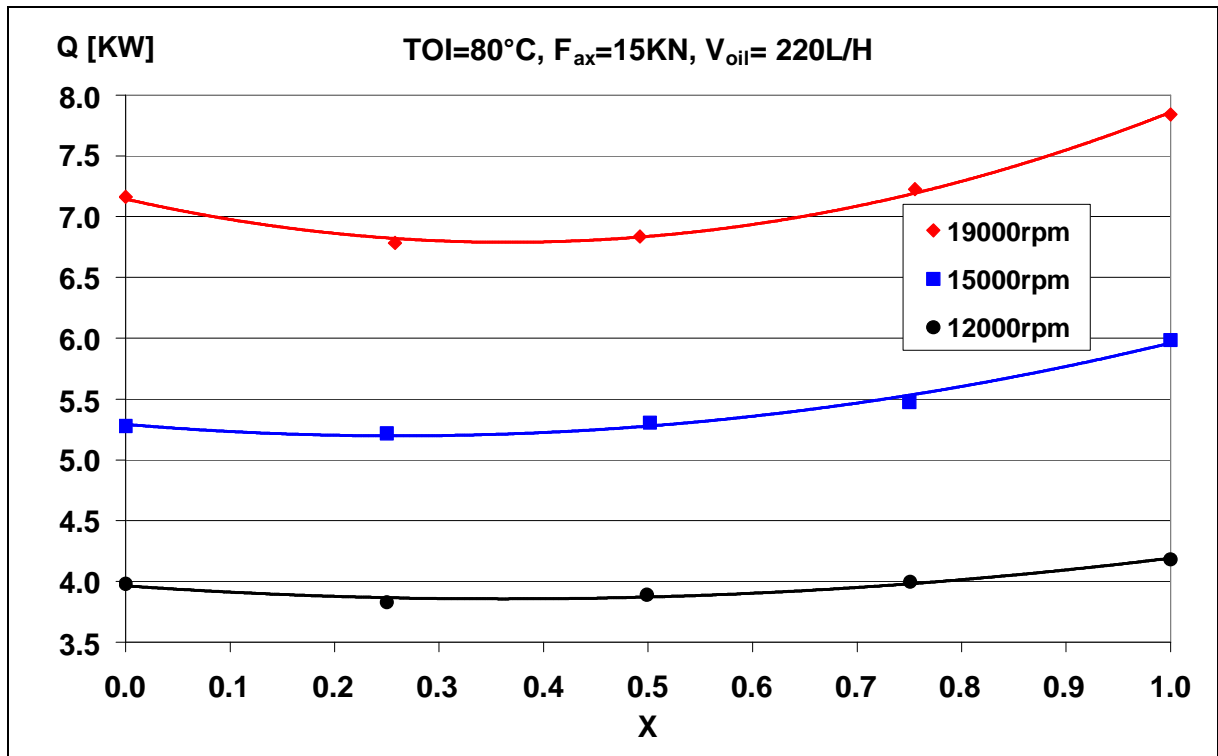


Figure 5. Bearing heat generation (Heat to Oil, Q) as a function of the oil flow ratio X at different rotational speeds

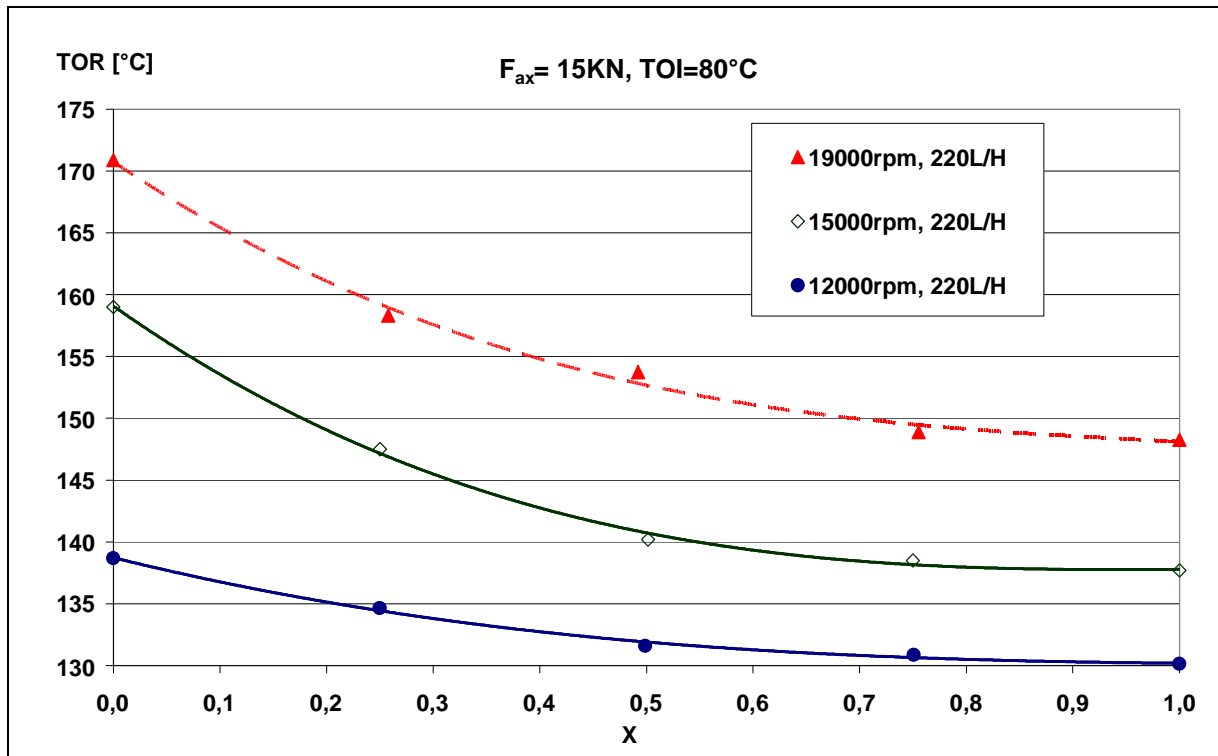


Figure 6. Outer Ring temperatures as a function of the oil flow ratio X at different rotational speeds

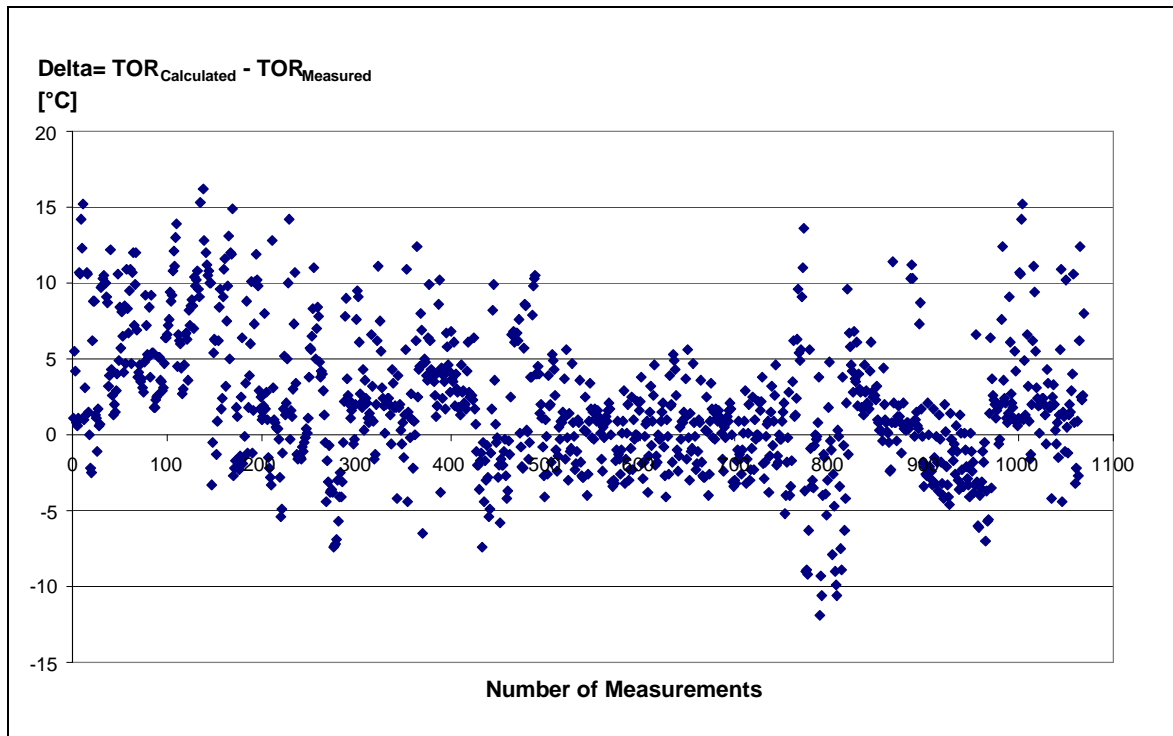


Figure 7. More than 92% of the measured points are in the $\pm 10^\circ\text{C}$ range of the calculated values using Equation 6.

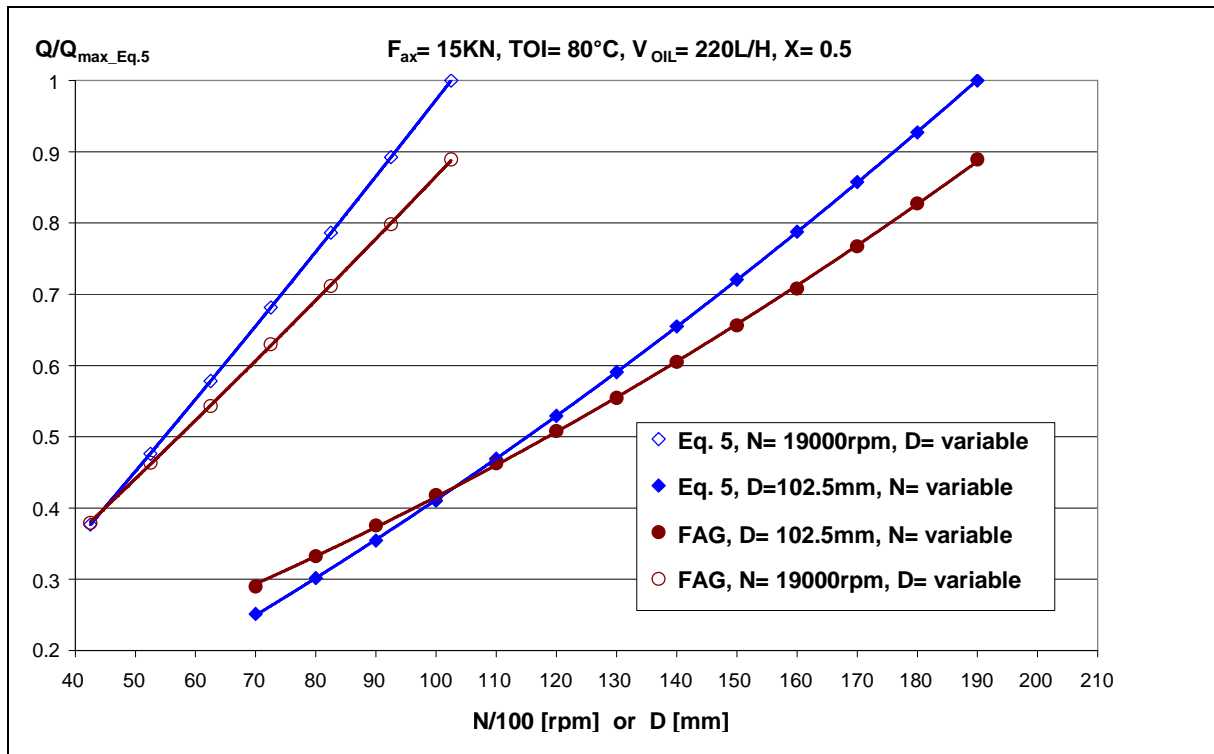


Figure 8. Variation of the heat generation as predicted by FAG Kugelfischer and calculated by Equation 5. The upper curves show the variation of the heat generation with the bore diameter of the bearing at 19000rpm whereas the lower curves show the variation of the heat generation with the rotational speed for a bearing of 102.5mm bore diameter.

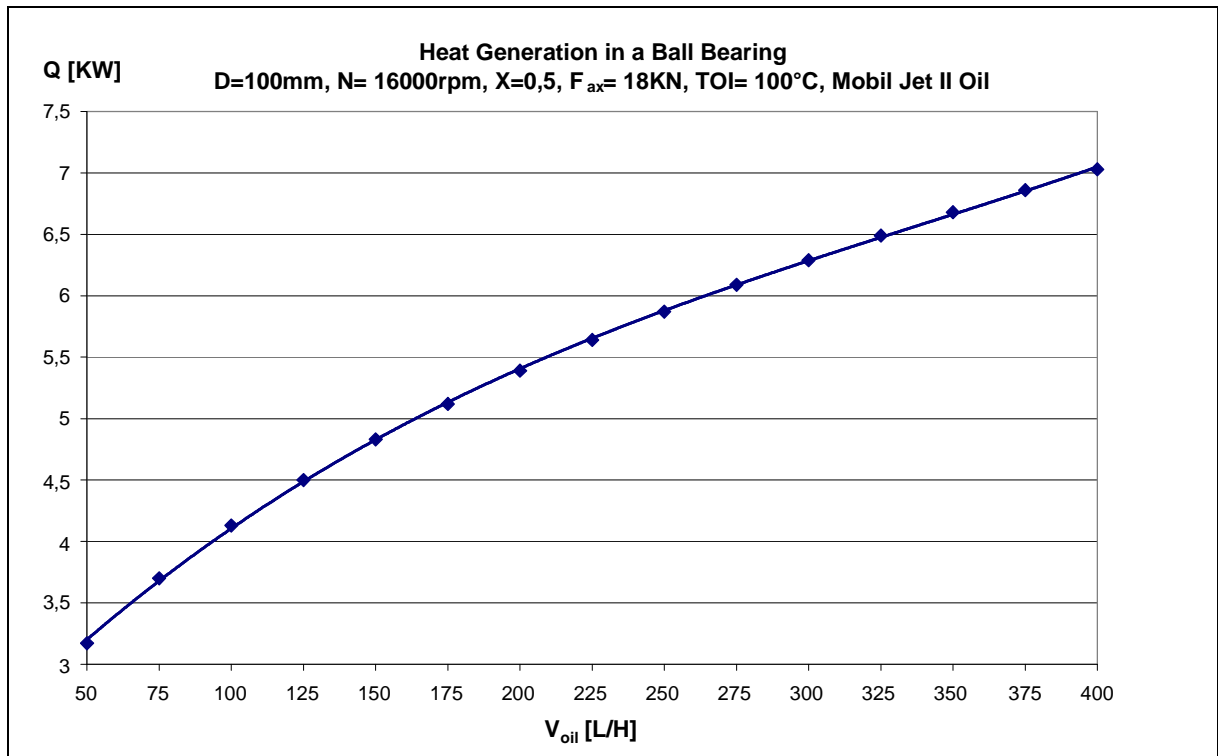


Figure 9. The Heat rejection into the oil from the bearing as a function of the oil flow

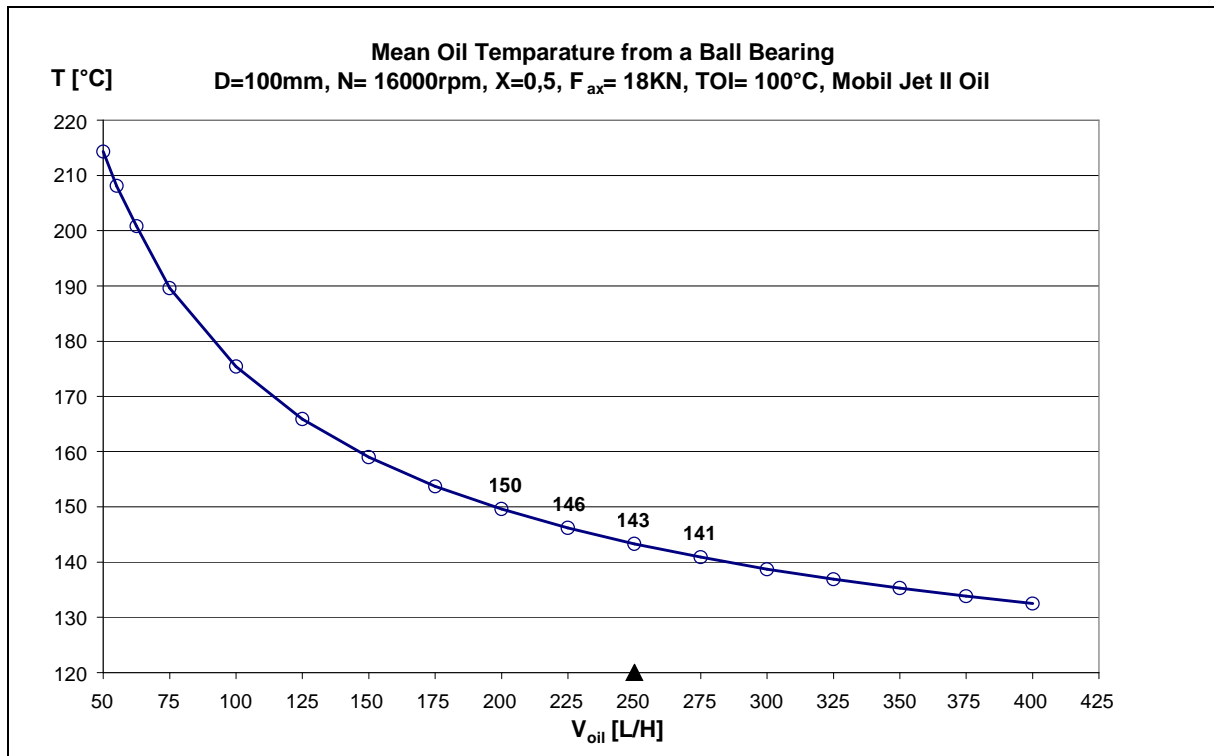


Figure 10. The mean oil temperature from the bearing as a function of the oil flow with the design point at 250L/H

19000rpm	Measurement	Equation 5		15000rpm	Measurement	Equation 5
X	Q [KW]	Q [KW]		X	Q [KW]	Q [KW]
0	7,16	7,31		0	5,28	5,27
0,25	6,78	7,12		0,25	5,22	5,13
0,5	6,84	7,16		0,5	5,31	5,16
0,75	7,23	7,42		0,75	5,47	5,35
1	7,84	7,89		1	5,98	5,69

Table 1. Comparison between measured and calculated **Heat to Oil** at two rotational speeds, 220L/H oil flow, 80°C oil inlet temperature and 15KN axial load (Figure 5)

12000rpm	Measurement	Equation 5
X	Q [KW]	Q [KW]
0	3,98	3,87
0,25	3,83	3,77
0,5	3,89	3,79
0,75	4,00	3,93
1	4,18	4,18

Table 2. Comparison between measured and calculated **Heat to Oil** at 12000rpm, 220L/H oil flow, 80°C oil inlet temperature and 15KN axial load (Figure 5)

19000rpm	Measurement	Equation 6
X	TOR [°C]	TOR [°C]
0	171	170
0,25	158	164
0,5	154	160
0,75	149	156
1	148	153

Table 3. Comparison between measured and calculated Outer Ring temperatures **TOR** at 19000rpm, 220L/H oil flow, 80°C oil inlet temperature and 15KN axial load (Figure 6)

15000rpm X	Measurement TOR [°C]	Equation 6 TOR [°C]		12000rpm X	Measurement TOR [°C]	Equation 6 TOR [°C]
0	159	152		0	139	137
0,25	148	147		0,25	135	134
0,5	140	143		0,5	132	131
0,75	139	140		0,75	131	128
1	138	137		1	130	126

Table 4. Comparison between measured and calculated Outer Ring temperatures TOR at 15000rpm and 12000rpm, 220L/H oil flow, 80°C oil inlet temperature and 15KN axial load (Figure 6)

	HTO Equation 1	TOR Equation 2
A	2,25	
B	-1,5068	
C	7,0221	
E	$1,5067 \cdot 10^{-9}$	
G		$1,1506 \cdot 10^{-3}$
α	1,11	
β	1,3855	
γ	0,0525	
δ	0,2152	
ε	0,3831	
ζ	0,761	
η		0,8729
θ		0,9876
κ		0,1234
λ		0,2469
μ		-0,3174
ξ		-0,3174

Table 5. The coefficients and exponents of the Heat to Oil and the Outer Ring Temperature polynomials